SZABO SCANDIC

Part of Europa Biosite

Produktinformation

- Forschungsprodukte & Biochemikalien
- Zellkultur & Verbrauchsmaterial
- Diagnostik & molekulare Diagnostik
- Laborgeräte & Service

Weitere Information auf den folgenden Seiten!
See the following pages for more information!

Lieferung & Zahlungsart

siehe unsere Liefer- und Versandbedingungen

Zuschläge

- Mindermengenzuschlag
- Trockeneiszuschlag
- Gefahrgutzuschlag
- Expressversand

SZABO-SCANDIC HandelsgmbH

Quellenstraße 110, A-1100 Wien

T. +43(0)1 489 3961-0

F. +43(0)1 489 3961-7

mail@szabo-scandic.com

www.szabo-scandic.com

linkedin.com/company/szaboscandic

Order online now!

www.rockland.com
tech@rockland.com
+1 484.791.3823

Datasheet for MB-070-003

Blocking Buffer for Fluorescent Western Blotting 3-PACK (3 x 500 ml)

Overview

Description:	Blocking Buffer for Fluorescent Western Blotting 3-PACK (3 x 500 ml) - MB-070-003
Item No.:	MB-070-003
Size:	3 x 500 mL
Applications:	WB, Cellular Assay, ELISA, IF, IHC, IP, Microarray, Other

Product Details

Background:	This blocking buffer is specifically designed for Western blotting using fluorochrome conjugated antibodies. Pure nitrocellulose membrane is recommended for maximum performance. Other membranes, such as PVDF or nitrocellulose embedded in a support can be used, but may generate elevated backgrounds. Protein should be transferred from gel to membrane using standard protocols. Blocking buffer can be used for membrane blocking and to dilute both primary and secondary antibodies. Blocking Buffer for Fluorescent Western Blotting is suitable for use with imaging systems produced by Bio-Rad Laboratories, GE Healthcare, Alpha Innotech, FujiFilm Life Science, Licor Biosciences, UVP and Syngene.
Synonyms:	Multiplex Blocking Buffer, Fluorescent Blocking Buffer, Blocking Solution, Blocking Buffer Western Blot, IRDye Western Blot Blocking Buffer, Alexa Dye Blocking Buffer, DyLight Blocking Buffer

Target Details

Purity/Specificity:	Blocking buffer was prepared using ultra pure reagents dissolved in pharmaceutical grade water (WFI) and consists of a proprietary protein formulation in TRIS buffered saline at pH 7.6 with thimerosal added as an antimicrobial agent.
Relevant Links:	• MB-070 SDS • PEPperCHIP Peptide Microarray Application Note

Application Details

Tested Applications:	WB
Suggested Applications:	Cellular Assay, ELISA, IF, IHC, IP, Microarray, Other (Based on references)

Application Note:	Fluorescence technology is widely used to detect proteins in both the visible and near-infrared ranges. This product allows for superior signal detection and lower background noise when fluorochrome conjugated antibodies are used to visualize proteins in Western blotting and other applications. Antibody conjugates prepared with IRDye® 800 and IRDye® 700DX, Cy2™, Cy3™, Cy3.5™, Cy5™ and Cy5.5™, DyLight™405, DyLight™ 549, DyLight™ 649, DyLight™ 680, and DyLight™ 800 and Alexa Fluor® 488, Alexa Fluor® 532, Alexa Fluor® 546, Alexa Fluor® 647 and Alexa Fluor® 680 have been validated on various platforms using this product with superior results compared to other commercially available products. In the infrared range, where little to no autofluorescence occurs, specific signal is sharply evident from any background giving the best possible signal-to-noise ratio. This allows for detection levels in the picogram range which rivals the sensitivity of chemiluminescence on film for Western blotting. Superior results are also seen when this product is used for simultaneous labeling (multiplex) in Western blots or microscopy using various fluorochrome combinations for multicolor imaging. Membranes blocked with this product can be dried and are very stable. Membranes that are stored protected from light can be re-washed and/or rescanned.
Assay Dilutions:	All assays should be optimized by the user. Recommended dilutions (if any) may be listed below.
WB:	User Defined

Formulation

Physical State:	Liquid (sterile filtered)
Concentration:	1X
Buffer:	See application note.
Preservative:	Thimerosal is added as an antimicrobial agent.

Shipping & Handling

Shipping Condition:	Wet Ice
Storage Condition:	Store blocking buffer at 4° C prior to opening. DO NOT FREEZE.
Expiration:	Expiration date is six (6) months from date of receipt.

Images

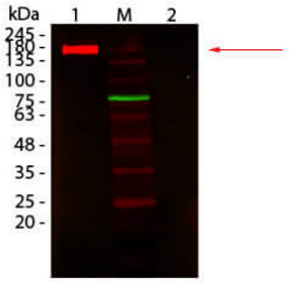

Western Blot
Western Blot of Fluorescent TrueBlot®: Anti-Rabbit IgG DyLight 680 Conjugated using MB-070.
Lane 1: Rabbit IgG, Non-denatured.
Lane 2: Rabbit IgG, Denatured.
Load: 50 ng per lane.
Primary antibody: none.
Secondary antibody: Fluorescent TrueBlot®: Anti-Rabbit IgG DyLight 680 Conjugated antibody at 1:1,000 for 60 min at RT.
Block: MB-070 for 30 min at RT.
Predicted: 160 kDa for non-denatured; observed: 170-180 kDa for non-denatured. Band migrates at slightly higher molecular weight.

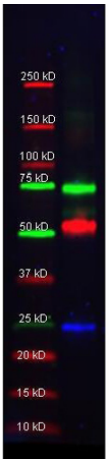

Western Blot
Multiplex western blot results using MB-070. Rockland Mouse-a-GST (200-301-200 lot 24882, blue), Rabbit anti-Transferrin (109-4134 lot 3033), and Goat-anti-Alpha-1-Anti-Trypsin (100-101-147 lot 5842) were used in a multiplex system to detect target proteins under reducing conditions in albumin depleted human serum with 320 ng of added GST. Sample was run by SDS-PAGE, transferred to 0.2 um PVDF using the BioRad Trans-Blot Turbo and blocked in 2.5% Blotto, 2.5% BSA, 0.02% Tween over night at 4°C. Membrane was probed with three primary antibodies at 1:1000 dilution (in MB-070 over night at 4°C). Detection shown was using DyLight™549 Donkey anti-Rabbit IgG (611-742-127 lot 21100, shown as green) DyLight™488 Donkey anti-Mouse IgG (610-741-124 lot 21095, shown as blue), and DyLight™649 Donkey anti-Goat IgG (605-743-125 lot 20834, shown as red) at 1:10,000 (in MB-070 at 30 min RT). Blots were washed, rinsed in methanol, dried and Images were collected using the BioRad VersaDoc System.

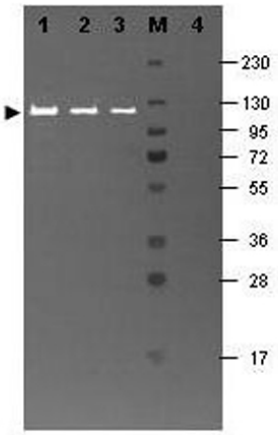

Western Blot
Western blot results using MB-070 and Fluorescein conjugated anti-b-Galactosidase antibody shows a band at ~117 kDa. Lanes 1 - 3 loaded with 60 ng, 30 ng and 15 ng, respectively of b-Gal present in partially purified preparations (arrowhead). Lane 4 shows no cross reactivity with proteins present in a non-specific control E.coli lysate. Proteins were resolved on a 4-20% Tris-Glycine gel by SDS-PAGE and transferred to nitrocellulose and blocking using Blocking Buffer for Fluorescent Western Blotting (p/n MB-070). The membrane was probed with fluorescein conjugated anti-b-Galactosidase (p/n 200-4236) diluted to 1:10,000. Reaction occurred for 2 hours at room temperature. Molecular weight estimation was made by comparison to a prestained MW marker in lane M. Fluorescence image was captured using the VersaDoc® Imaging System developed by BIO-RAD. Other detection systems will yield similar results.

Dot Blot
Dot Blot of Human IgA Fluorescein using MB-070.
Antigen: Human IgA Fluorescein.
Load: 3-fold serial dilution starting at 200 ng.
Block: MB-070 for 30 min at RT.

Example of stained microarray

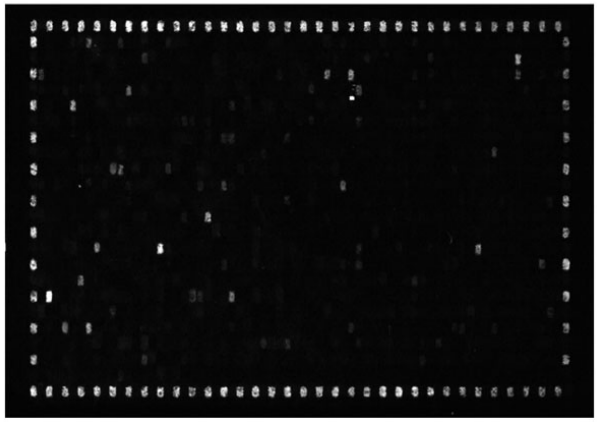

Figure
702 Peptides are printed in duplicates randomly distributed on the microarray. Control peptides (HA and FLAG controls) are located in a square surrounding the peptides of interest. As secondary antibody DyLight™ 549 conjugated goat anti-human IgG antibody and for the FLAG control peptide a mouse anti-FLAG-Cy3 antibody were used; microarrays were read using a Fujifilm Life Science FLA-5100 imaging system with a SHG 532nm (green) diode laser and an LPG filter. Fig e1. PMID: 26894206.

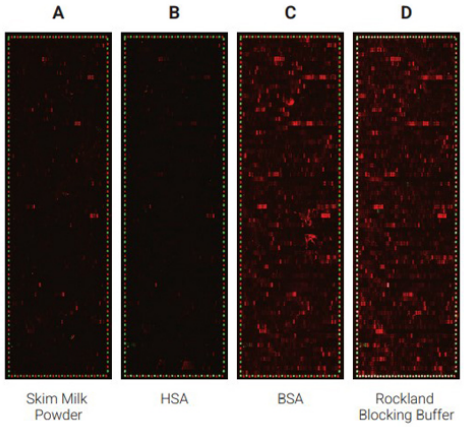

Comparison of the performance of different blocking reagents in epitope mappings with PEPperCHIP® Peptide Microarrays.
The PEPperCHIP® Peptide Microarrays were blocked for 30 minutes with either 2% skim milk powder (A), 1% HSA (B), 1% BSA (C) or 100% Rockland Blocking Buffer [p/n MB-070] (D). A human serum sample was assayed at dilution 1:200, followed by detection with secondary goat anti-Human IgG (H+L) DyLight™ 680 Antibody [p/n 609-144-123] and a control anti-HA (12CA5)-DyLight™ 800 Antibody. Red spots = sample IgG response and frame of polio control peptides, green spots = frame of HA control peptides.

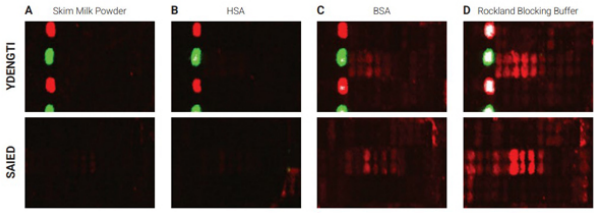

Selected sections of the PEPperCHIP® Peptide Microarrays after assay with different blocking reagents. The microarrays were blocked for 30 minutes with either 2% skim milk powder (A), 1% HSA (B), 1% BSA (C) or 100% Rockland Blocking Buffer [p/n MB-070] (D), respectively. A human serum sample was assayed at dilution 1:200, followed by detection with secondary goat Anti-Human IgG (H+L) DyLight™ 680 Antibody [p/n 609-144-123]. Red spots = sample responses and polio control peptides, green spots = HA control peptides. The underlying binding motifs of the respective sections are indicated on the left.

Bottle
Blocking Buffer for Fluorescent Western Blotting

References

- Rebak AS et al. A quantitative and site-specific atlas of the citrullinome reveals widespread existence of citrullination and insights into PADI4 substrates. *Nat Struct Mol Biol.* (2024)
- Gaudet ID et al. Elevated SLC7A2 expression is associated with an abnormal neuroinflammatory response and nitrosative stress in Huntington's disease. *J Neuroinflammation.* (2024)
- Dossat AM et al. Excitotoxic glutamate levels cause the secretion of resident endoplasmic reticulum proteins. *J Neurochem.* (2024)
- Rosenkranz M et al. Full-length MSP1 is a major target of protective immunity after controlled human malaria infection. *Life Sci Alliance.* (2024)
- Mashayekhi V et al. The RNA binding protein IGF2BP2/IMP2 alters the cargo of cancer cell-derived extracellular vesicles supporting tumor-associated macrophages. *Cell Commun Signal.* (2024)
- Ampudia-Mesias E et al. The OTX2 Gene Induces Tumor Growth and Triggers Leptomeningeal Metastasis by Regulating the mTORC2 Signaling Pathway in Group 3 Medulloblastomas. *Int J Mol Sci.* (2024)
- Kokic G et al. Structural basis for RNA polymerase II ubiquitylation and inactivation in transcription-coupled repair. *Nat Struct Mol Biol.* (2024)
- Takahashi H et al. Reduced progranulin increases tau and α-synuclein inclusions and alters mouse tauopathy phenotypes via glucocerebrosidase. *Nat Commun.* (2024)
- Croote D et al. Widespread monoclonal IgE antibody convergence to an immunodominant, proanaphylactic Ara h 2 epitope in peanut allergy. *J Allergy Clin Immunol.* (2024)
- Frische A et al. Antigen-Heterologous Vaccination Regimen Triggers Alternate Antibody Targeting in SARS-CoV-2-DNA-Vaccinated Mice. *Vaccines (Basel).* (2024)
- Desmet C et al. ASFV epitope mapping by high density peptides microarrays. *Virus Res.* (2024)
- Stoner A et al. Neuronal transcriptome, tau and synapse loss in Alzheimer's knock-in mice require prion protein. *Alzheimers Res Ther.* (2023)
- Cecchini K et al. The transcription factor TCFL5 responds to A-MYB to elaborate the male meiotic program in mice. *Reproduction.* (2023)
- Hsueh HT et al. Machine learning-driven multifunctional peptide engineering for sustained ocular drug delivery. *Nat Commun.* (2023)
- Vengesai A et al. Peptide microarray analysis of in-silico predicted B-cell epitopes in SARS-CoV-2 sero-positive healthcare workers in Bulawayo, Zimbabwe. *Acta Trop.* (2023)
- Barrett MR et al. Conditioning-induced expression of novel glucose transporters in canine skeletal muscle homogenate. *PLoS One.* (2023)
- Tingstedt JL et al. Differential recognition of influenza A virus H1N1 neuraminidase by DNA vaccine-induced antibodies in pigs and ferrets. *Front Immunol.* (2023)
- Sekine Y et al. Amino-terminal proteolytic fragment of the axon growth inhibitor Nogo-A (Rtn4A) is upregulated by injury and promotes axon regeneration. *J Biol Chem.* (2023)
- Frische A et al. A Candidate DNA Vaccine Encoding the Native SARS-CoV-2 Spike Protein Induces Anti-Subdomain 1 Antibodies. *Vaccines (Basel).* (2023)

- Zhang T et al. A zebrafish model of combined saposin deficiency identifies acid sphingomyelinase as a potential therapeutic target. *Dis Model Mech.* (2023)
- Kanashiro-Takeuchi RM et al. Efficacy of a growth hormone-releasing hormone agonist in a murine model of cardiometabolic heart failure with preserved ejection fraction. *Am J Physiol Heart Circ Physiol.* (2023)
- Xu H et al. Characterization of huntingtin interactomes and their dynamic responses in living cells by proximity proteomics. *J Neurochem.* (2023)
- Acharjee A et al. Humoral Immune Response Profile of COVID-19 Reveals Severity and Variant-Specific Epitopes: Lessons from SARS-CoV-2 Peptide Microarray. *Viruses.* (2023)
- Figo DD et al. IgE and IgG4 Epitopes of Dermatophagoides and Blomia Allergens before and after Sublingual Immunotherapy. *Int J Mol Sci.* (2023)
- Prudencio CR et al. Identification of Zika Virus NS1-Derived Peptides with Potential Applications in Serological Tests. *Viruses.* (2023)
- Russo G et al. In vitro evolution of myc- tag antibodies: in-depth specificity and affinity analysis of Myc1-9E10 and Hyper-Myc. *Biol Chem.* (2022)
- Gibb AA et al. Glutamine uptake and catabolism is required for myofibroblast formation and persistence. *J Mol Cell Cardiol.* (2022)
- Arif A et al. GTSF1 accelerates target RNA cleavage by PIWI-clade Argonaute proteins. *Nature.* (2022)
- Blessing, C et al. XPC-PARP complexes engage the chromatin remodeler ALC1 to catalyze global genome DNA damage repair. *Nature Communications* (2022)
- Vengesai, A et al. Multiplex peptide microarray profiling of antibody reactivity against neglected tropical diseases derived B-cell epitopes for serodiagnosis in Zimbabwe. *PloS One* (2022)
- Fahnoe, KC et al. Development and Optimization of Bifunctional Fusion Proteins to Locally Modulate Complement Activation in Diseased Tissue. *Frontiers in Immunology* (2022)
- Gopalakrishnan, S et al. Tofacitinib Downregulates TNF and Poly(I:C)-Dependent MHC-II Expression in the Colonic Epithelium. *Frontiers in Immunology* (2022)
- Metselaar, DS et al. AURKA and PLK1 inhibition selectively and synergistically block cell cycle progression in diffuse midline glioma. *IScience* (2022)
- Adel, M et al. Pairing-Dependent Plasticity in a Dissected Fly Brain Is Input-Specific and Requires Synaptic CaMKII Enrichment and Nighttime Sleep. *The Journal of Neuroscience : the Official Journal of the Society for Neuroscience* (2022)
- Parsons, AJ et al. Development of broadly neutralizing antibodies targeting the cytomegalovirus subdominant antigen gH. *Communications Biology* (2022)
- D'alessandro-Gabazza, CN et al. Inhibition of lung microbiota-derived proapoptotic peptides ameliorates acute exacerbation of pulmonary fibrosis. *Nature Communications* (2022)
- Frankel, D et al. miR-376a-3p and miR-376b-3p overexpression in Hutchinson-Gilford progeria fibroblasts inhibits cell proliferation and induces premature senescence. *IScience* (2022)
- Mantsounga, CS et al. Macrophage IL-1β promotes arteriogenesis by autocrine STAT3- and NF-κB-mediated transcription of pro-angiogenic VEGF-A. *Cell Reports* (2022)

- Yu T et al. A-MYB/TCFL5 regulatory architecture ensures the production of pachytene piRNAs in placental mammals. *RNA.* (2022)
- Paris G et al. Automated Laser-Transfer Synthesis of High-Density Microarrays for Infectious Disease Screening. *Adv Mater.* (2022)
- Lucchese G et al. Anti-neuronal antibodies against brainstem antigens are associated with COVID-19. *EBioMedicine.* (2022)
- Bell CJ et al. Novel colchicine derivative CR42-24 demonstrates potent anti-tumor activity in urothelial carcinoma. *Cancer Lett.* (2022)
- Rashid FZM et al. HI-NESS: a family of genetically encoded DNA labels based on a bacterial nucleoid-associated protein. *Nucleic Acids Research* (2022)
- Garbincius JF et al. Enhanced NCLX-dependent mitochondrial Ca2+ efflux attenuates pathological remodeling in heart failure. *J Mol Cell Cardiol.* (2022)
- Solis O et al. The SARS-CoV-2 spike protein binds and modulates estrogen receptors. *Sci Adv.* (2022)
- Sekine Y et al. Rabphilin3A reduces integrin-dependent growth cone signaling to restrict axon regeneration after trauma. *Exp Neurol.* (2022)
- Chapman JH et al. UPF1 mutants with intact ATPase but deficient helicase activities promote efficient nonsense-mediated mRNA decay. *Nucleic Acids Res.* (2022)
- Garcia-Montojo M et al. Antibody Response to HML-2 May Be Protective in Amyotrophic Lateral Sclerosis. *Ann Neurol.* (2022)
- Tomer D et al. A new mechanism of fibronectin fibril assembly revealed by live imaging and super-resolution microscopy. *J Cell Sci.* (2022)
- View More ...

Disclaimer

This product is for research use only and is not intended for therapeutic or diagnostic applications. Please contact a technical service representative for more information. All products of animal origin manufactured by Rockland Immunochemicals are derived from starting materials of North American origin. Collection was performed in United States Department of Agriculture (USDA) inspected facilities and all materials have been inspected and certified to be free of disease and suitable for exportation. All properties listed are typical characteristics and are not specifications. All suggestions and data are offered in good faith but without guarantee as conditions and methods of use of our products are beyond our control. All claims must be made within 30 days following the date of delivery. The prospective user must determine the suitability of our materials before adopting them on a commercial scale. Suggested uses of our products are not recommendations to use our products in violation of any patent or as a license under any patent of Rockland Immunochemicals, Inc. If you require a commercial license to use this material and do not have one, then return this material, unopened to: Rockland Inc., P.O. BOX 5199, Limerick, Pennsylvania, USA.